Biomechanical Regulation of Endothelial Phenotype

Lee, Ee Soo

Chapter 2

Endothelial-to-mesenchymal transition contributes to fibro-proliferative vascular disease and is modulated by fluid shear stress

Jan-Renier A.J. Moonen[1], Ee Soo Lee[1], Marc Schmidt[2], Monika Maleszewska[1], Jasper A. Koerts[1], Linda A. Brouwer[1], Theo G. van Kooten[3], Marja J.A. van Luyn[1], Clark J. Zeebregts[4], Guido Krenning[1] and Martin C. Harmsen[1]

[1]University of Groningen, University Medical Center Groningen, Department of Pathology and Medical Biology, Groningen, The Netherlands.
[2]University of Wuerzburg, Department of Dermatology, Venerology and Allergology, Wuerzburg, Germany.
[3]University of Groningen, University Medical Center Groningen, Department of Biomedical Engineering, Groningen, The Netherlands.
[4]University of Groningen, University Medical Center Groningen, Department of Surgery, Division of Vascular Surgery, Groningen, The Netherlands.

Cardiovascular Research. 2015; doi:10.1093/cvr/cvv175. [Epub ahead of print]

Abstract

Aims:

Neointimal hyperplasia is a common feature of fibro-proliferative vascular disease and characterizes initial stages of atherosclerosis. Neointimal lesions are mainly comprised of smooth muscle-like cells. The presence of these lesions is related to local differences in shear stress. Neointimal cells may arise through migration and proliferation of smooth muscle cells from the media. However, a role for the endothelium as a source of smooth muscle-like cells has largely been disregarded. Here, we investigated the role of endothelial-to-mesenchymal transition (EndMT) in neointimal hyperplasia and atherogenesis, and studied its modulation by shear stress.

Methods and results:

In human atherosclerotic plaques and porcine aortic tissues, myo-endothelial cells were identified, suggestive for EndMT. Flow disturbance by thoracic-aortic constriction in mice, similarly showed presence of myo-endothelial cells, specifically in regions exposed to disturbed flow. While uniform laminar shear stress (LSS) was found to inhibit EndMT, endothelial cells exposed to disturbed flow underwent EndMT, *in vitro* and *in vivo*, and showed atherogenic differentiation. Gain- and loss-of-function studies using a constitutive active mutant of MEK5 and short hairpins targeting ERK5 established a pivotal role for ERK5 signalling in the inhibition of EndMT.

Conclusions:

Together, these data suggest that EndMT contributes to neointimal hyperplasia and induces atherogenic differentiation of endothelial cells. Importantly, we uncovered that EndMT is modulated by shear stress in an ERK5-dependent manner. These findings provide new insights in the role of adverse endothelial plasticity in vascular disease and identify a novel atheroprotective mechanism of uniform LSS, namely inhibition of EndMT.

Introduction

Neointimal hyperplasia is a common feature of fibro-proliferative vascular disease and characterizes initial stages of atherosclerosis, a multifactorial disease that primarily affects large- and medium-sized arteries.[1] Although most risk factors for atherosclerosis are present at the systemic level, the disease develops in predisposed, atheroprone regions.[2] These regions are characterized by disturbed flow, typically encountered at the outer walls of vascular bifurcations and at the inner wall of vascular curvatures.[3] Previous studies have identified anti-inflammatory and anti-coagulant effects of uniform laminar shear stress (LSS) on endothelial cells (EC).[2,4] Besides, shear stress affects endothelial control of smooth muscle cell migration and proliferation.[5] We and others have previously shown that EC can acquire a fibro-proliferative mesenchymal phenotype through endothelial-to-mesenchymal transition (EndMT).[6-9] This transition process is characterized by loss of cell–cell adhesions and changes in cell polarity. Endothelial cell markers, such as VE-cadherin and PECAM-1 are reduced, while the expression of mesenchymal cell markers, such as α-smooth muscle actin (αSMA) and calponin are induced.[6,8] Functionally, cells acquire myofibroblast-like characteristics with contractile function, enhanced migratory phenotype, and increased extracellular matrix production.[8] In the process, endothelial function, such as anti-thrombogenicity, is lost.[6,8] EndMT was originally observed during embryogenesis where it plays a crucial role in cardiac valve formation.[10] In recent years, it has become clear that mesenchymal transition of EC is not restricted to embryonic development but also occurs in adult life, where it contributes to pulmonary vascular remodelling[11] and cardiac and kidney fibrosis.[12,13] In addition, EndMT has been suggested to occur in neointimal thickening associated with transplant atherosclerosis and restenosis.[14,15] The aims of this study were to elucidate whether EndMT contributes to neointimal hyperplasia and atherogenesis, and to decipher whether modulation of EndMT by fluid shear stress can explain the focal nature of fibro-proliferative vascular disease.

Materials and methods

Clinical samples

Carotid plaques were obtained from six patients undergoing elective carotid endarterectomy for symptomatic high-grade stenosis of the internal carotid artery at the department of Vascular Surgery, University Medical Center Groningen (UMCG). Samples were fixed in neutral buffered formalin prior to paraffin embedding. Patients gave informed consent and the investigation was performed according to institutional guidelines and the Declaration of Helsinki.

Animals and surgical procedures

Pigs

The investigation conforms to the recommendations in the 8th Edition of the Guide for the Care and Use of Laboratory Animals of the National Institutes of Health (NRC 2011) and was approved by the local Ethical Committee. Porcine abdominal aortic trifurcations were obtained from healthy male Yorkshire pigs (12–13 weeks of age; body weight 30–35 kg, n=3) which were obtained from V.O.F. van Beek (Lelystad, The Netherlands). Animals were fed a normal diet. Animals were sacrificed under anaesthesia with ketamine (Nimatek) and midazolam with a bolus of pentobarbital and heparin (Actrapid).

Mice

The investigation conforms to the recommendations in the 8th Edition of the Guide for the Care and Use of Laboratory Animals of the National Institutes of Health (NRC 2011) and was approved by the local Ethical Committee. Male C57Bl/6j wild-type mice (8–12 weeks of age, n=8) were obtained from Harlan (Horst, The Netherlands). During the entire experiment, animals were kept on a 12 h light:12 h dark cycle with ad libitum access to standard laboratory chow and water. Aortic banding (n=5) was performed under anaesthesia [2% Isofluorane (Forene/Abbott, The Netherlands) and oxygen] and analgesia (Carprofen, 5 mg/kg), with body temperature and hydration control throughout surgery. Briefly, an incision was made in the second intercostal space. Next, a small incision was made in the parietal pleura, through which the ascending loop of the aorta was exposed. A suture was placed around the aorta. The aorta was supported with a 27G needle, and suture was drawn tight, after which the needle was removed. Thereafter, the pleura, muscle layers, and skin were closed by sutures. Animals received post-operative analgesia (Carprofen, 5 mg/kg/24 h for 48 h). In sham-operated animals (n=3), all procedures were performed except for the actual aortic banding. Animals were sacrificed under deep anaesthesia [3% Isofluorane (Forene/Abbott, The Netherlands] by exsanguination, 8 weeks after the procedure, after which the thoracic aorta was explanted.

Cell cultures

Human umbilical vein endothelial cells (HUVEC) and human aortic endothelial cells (HAEC) were purchased from Lonza Walkersville (MD, USA) or obtained from the endothelial cell facility, UMCG and cultured in endothelial cell medium (ECM) up to passage 5 as described previously.[6] EndMT was initiated by culturing the cells in RPMI 1640 with 20% v/v foetal bovine serum (FBS), 1% v/v penicillin–streptomycin, 2 mM L-glutamine, 5 U mL^{-1} heparin, with addition of 5 ng mL^{-1} transforming growth factor β1 (TGFβ1) (Peprotech, NJ, USA). To study calcium deposition, cells were cultured in osteogenic medium consisting of DMEM/F12 with 10% v/v FBS,

1% v/v penicillin–streptomycin, 5 ng mL^{-1} TGFβ1, 100 nM dexamethasone, 10 mM β-glycerophosphate, and 100 μM of ascorbic acid. For shear stress experiments, HUVEC or HAEC were seeded on fibronectin-coated (1.5 μg cm^{-2}; Harbor Bio-Products, MA, USA) flow chamber slides, *i.e.* μ-Slide I or μ-Slide Y-shaped (ibiTreat; Ibidi, Germany) and grown to confluence before exposure to 20 dyne cm^{-2} of unidirectional uniform LSS. LSS was generated using the Ibidi Pump System (Ibidi, Germany). For static experiments, performed simultaneously with the shear stress experiments, HUVEC or HAEC were seeded on fibronectin-coated (1.5 mg cm^{-2}; Harbor Bio-Products) six-well culture plates (Greiner Bio One, The Netherlands).

Plasmids, lentiviral, and retroviral transductions

A retroviral construct for stable expression of constitutively active rat MEK5-α1 (pBP-MEK5D) was generated as described before.[23] For lentiviral expression of small hairpin RNA (shRNA) against ERK5, a 63-mer DNA oligonucleotide containing the specific 21-mer targeting sequence AAGCACTTTAAACACGACAAC for human Erk5 was cloned into the *BamHI/EcoRI* sites of the pGreenPuro shRNA expression vector (Systems Bioscience, CA, USA). A negative control shRNA sequence GATTCCAGACGTAGGCTTATAT was used as a control. Retroviral transduction of HUVEC and HAEC was performed as detailed before.[23] For lentiviral transductions, HEK293T cells were transfected with pGreenPuro shuttle vectors and second-generation lentiviral helper plasmids using Endofectin (GeneCopoeia, MD, USA). Viral supernatants were collected every 12–16 h, supplemented with 6 μg mL^{-1} polybrene and directly transferred to HUVEC cultures, starting from 24 h post-transfection for three consecutive rounds. Transduced cells were selected for puromycin resistance 72 h post-infection (2 μg mL^{-1} puromycin, 24 h) and reseeded into puromycin-free medium for the experiments.

Immunohistochemistry

Heat-induced epitope retrieval was performed with 0.1 M Tris–HCl (pH 9.0, 80°C, overnight) on the formalin fixated, paraffin-embedded sections before proceeding with immunohistochemistry. Sections were incubated with primary antibodies at 4°C overnight, followed by incubation with secondary antibodies at room temperature for 1 h. For calcium deposition, slides were incubated with Alizarin Red (Sigma-Aldrich, The Netherlands) at 20 mg mL^{-1}, pH 4.1. The list of antibodies and the used concentrations is provided in Supplementary materials, Table S1. Detailed description of the imaging procedures is provided in Supplementary materials, Methods.

Immunoblotting

Whole cell lysates were prepared in RIPA buffer (Thermo Scientific, IL, USA) supplemented with 1% protease inhibitor cocktail and 1% phosphatase inhibitor cocktail (both Sigma-Aldrich). Protein concentrations were determined using Bio-Rad DC protein assay (Bio-Rad, VA, USA), according to manufacturer's protocol. Equal amounts of protein were loaded on a 10% denaturing SDS–polyacrylamide gel, separated by gel electrophoresis and blotted onto nitrocellulose membrane (Hybond-P; Amersham Pharmacia Biotech, England, UK) according to standard protocols. Blots were blocked in Odyssey Blocking Buffer (Li-COR Biosciences, NE, USA) at room temperature for 1 h and incubated at 4^{o}C overnight with primary antibodies in Odyssey Blocking Buffer, supplemented with 0.1% Tween-20. Blots were incubated with secondary antibodies the next day. Protein was detected using the Odyssey Infrared Imaging System (Li-COR Biosciences). Densitometric analysis was performed using Totallab 120 (Nonlinear Dynamics, Newcastle upon Tyne, England). The list of employed antibodies and their concentrations is given in Supplementary materials, Table S2.

Gene transcript analysis

RNA was isolated using TRIzol reagent (Invitrogen Corp, CA, USA) according to the manufacturer's protocol. cDNA synthesis was performed using RevertAid^{TM} First Strand cDNA Synthesis Kit (Thermo Scientific, MA, USA), according to the manufacturer's protocol. The cDNA-equivalent of 5 ng RNA was used for amplification in 384-well microtitre plates in an ABI7900HT cycler (Applied Biosystems, CA, USA) using SYBR Green chemistry (Bio-Rad, VA, USA). Cycle threshold (Ct) values for individual reactions were determined using ABI Prism SDS 2.2 data processing software (Applied Biosystems) and normalized against β2M expression. All cDNA samples were amplified in duplicate. Relative expression was calculated using the ΔCt method. Data are presented as fold change compared with control, obtained using the ΔΔCt method. The list of primers (Biolegio, The Netherlands) is enclosed as Supplementary materials, Table S3.

Statistical analysis

Data are presented as means±standard error of the mean (SEM) n values relate to independent experiments. *P*-values were calculated using one-way analysis of variance followed by Bonferroni's *post-hoc* comparisons tests using Graphpad Prism (Graphpad Software, La Jolla, CA, USA). $P < 0.05$ was considered statistically significant.

Results

Human atherosclerotic plaques were analysed for co-expression of platelet endothelial cell adhesion molecule-1 (PECAM-1), and mesenchymal marker αSMA. Double-positive cells were detected, suggestive for cells in intermediate stages of EndMT, both in the inner lining as well as deeper in the neointimal tissue (Figure 1A). Given the focal nature of vascular disease, we next evaluated whether the presence of EndMT was related to local differences in shear stress profiles. Since complete transition results in loss of classical endothelial markers, the expression of endocan was analysed, an endothelial dermatan sulphate proteoglycan also known as endothelial specific molecule-1, which co-expresses with mesenchymal markers during embryonic EndMT.[16] We investigated regions exposed to uniform LSS and disturbed flow in the porcine abdominal aortic trifurcation (Figure 1B and Supplementary materials,

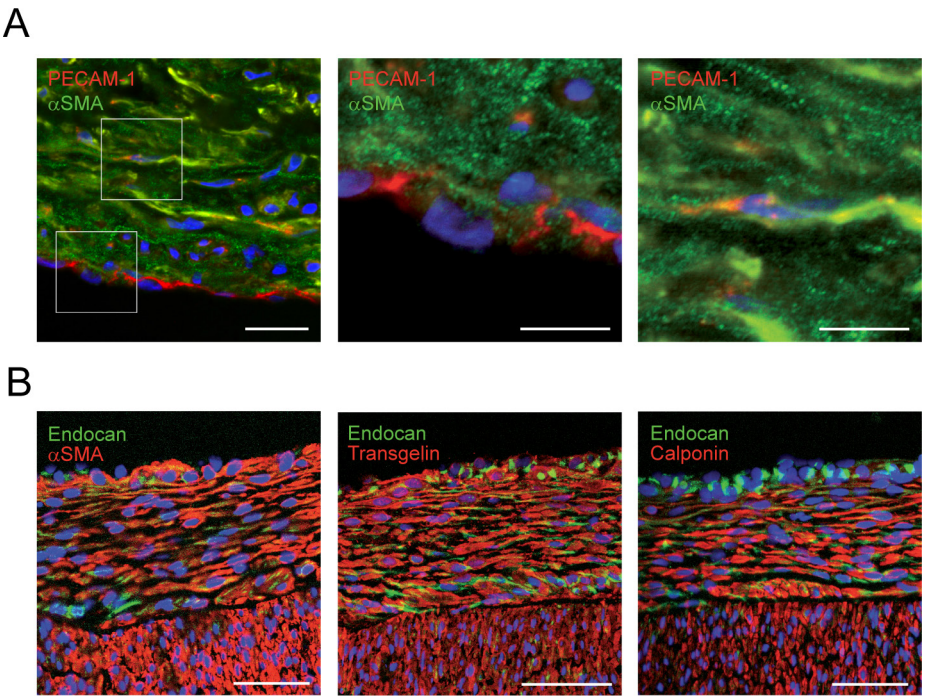

Figure 1. Atherosclerotic plaques and neointimal lesions contain myo-EC. (A) Confocal images of a representative human atherosclerotic plaque show cells co-expressing PECAM-1 (red) and mesenchymal marker αSMA (green). Nuclei are stained with DRAQ5 (blue). n=6. Scale bars: 25 and 10 µm for magnification. **(B)** Representative confocal images of neointimal lesions of the outer walls of the porcine trifurcation, show myo-EC co-expressing endocan (green) and mesenchymal markers αSMA, transgelin and calponin (all in red). Nuclei are stained with DAPI (blue). n=3. Scale bars: 50 µm.

Figure S1). The outer walls of the trifurcation, characterized by disturbed flow,[17] showed pronounced neointimal thickening. Endocan-positive cells were detected throughout the neointima and co-expressed mesenchymal markers αSMA, transgelin, and calponin (Figure 1B and Supplementary materials, Figure S1A). In contrast, neointimal lesions were absent in areas exposed to uniform LSS, and endocan expression was confined to the endothelial monolayer (Supplementary materials, Figure S1B).

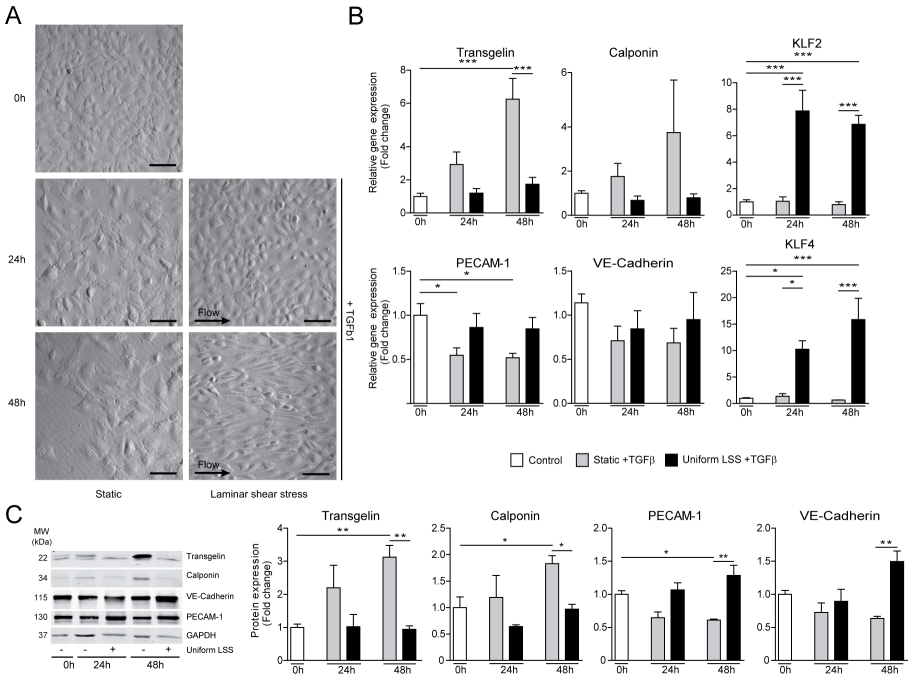

Figure 2. Uniform LSS inhibits endothelial-to-mesenchymal transition. (A) Phase contrast images of HUVEC stimulated with 5 ng mL^{-1} TGFβ1, both under static conditions and with concomitant exposure to 20 dyne cm^{-2} of uniform LSS for 24 and 48 h. Scale bars: 10 μm. **(B)** Mesenchymal and endothelial gene expression levels were determined by quantitative RT-PCR, and expression was related to untreated control HUVEC. Under static conditions, expression of transgelin is increased while PECAM-1 shows reduced expression levels. Relative gene expression levels of KLF2 and KLF4 were induced by exposure to LSS at 24 and 48 h. n=6. **(C)** Representative immunoblots and quantification of mesenchymal proteins transgelin and calponin and endothelial proteins VE-Cadherin and PECAM-1 of untreated HUVEC (0 h) and HUVEC stimulated with 5 ng ml^{-1} TGFβ1, both under static conditions (–) and with concomitant exposure to 20 dyne cm^{-2} of uniform LSS (+) for 24 and 48 h. n=3. *P* values were calculated using one-way ANOVA followed by Bonferroni's post-hoc comparisons tests. * $P < 0.05$, ** $P < 0.01$, and *** $P < 0.001$.

Since regions exposed to uniform LSS showed no evidence for the presence of myo-EC, suggesting protection from EndMT, the effect of uniform LSS was studied on EndMT *in vitro*. HUVEC were stimulated with TGFβ1, both under static conditions and with exposure to 20 dyne cm^{-2} of uniform LSS, comparable to the average level of shear stress found in large arteries.[18] Under static conditions, stimulation with TGFβ1 resulted in hypertrophy and disruption of the monolayer, similar to earlier descriptions of embryonic EndMT[19] (Figure 2A). In contrast, when cells were stimulated with TGFβ1 and concomitantly exposed to uniform LSS, they aligned to the flow direction, and retained a confluent monolayer (Figure 2A). In the absence of uniform LSS, EndMT was induced, confirmed by the induction of mesenchymal markers on gene-transcript levels (Figure 2B) and protein expression levels (Figure 2C). Endothelial PECAM-1 expression levels were reduced on gene-transcript and protein-expression levels (Figure 2B and C). VE-Cadherin expression levels showed a similar trend but were not significantly changed, this is likely explained by the limited timeframe in which the experiments were performed, as waning of endothelial markers follows the induction of mesenchymal markers during the transition process. Cells exposed to uniform LSS maintained the endothelial phenotype and thus were resistant to EndMT (Figure 2B and C). To confirm that uniform LSS also inhibits EndMT of adult EC, HAEC were similarly stimulated with TGFβ1, both under static conditions and with concomitant exposure to 20 dyne cm^{-2} of uniform LSS. As expected, stimulation of HAEC with TGFβ1 under static conditions induced EndMT, which was inhibited by uniform LSS (Supplementary materials, Figure S2A).

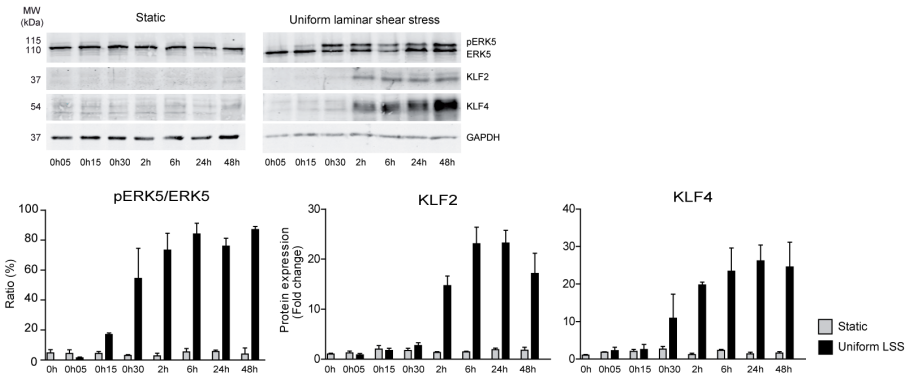

Figure 3. Uniform LSS induces sustained activation of ERK5. HUVEC were exposed to 20 dyne cm^{-2} of LSS for up to 48 h. Activation status, *i.e.* phosphorylation of ERK5 was determined at the indicated time points by immunoblotting. Representative immunoblots and quantification of LSS-induced activation of ERK5 and expression of downstream effectors KLF2 and KLF4. n=3.

Next, we dissected the pathway responsible for inhibition of EndMT by uniform LSS. While all major MAPK pathways are involved in mechanotransduction of shear stress, a major role is accredited to the MEK5/ERK5 cascade[20] and many of the atheroprotective effects of uniform LSS have been attributed to this signalling cascade.[20-22] In contrast to other MAPK signalling pathways, which showed transient activation upon exposure to

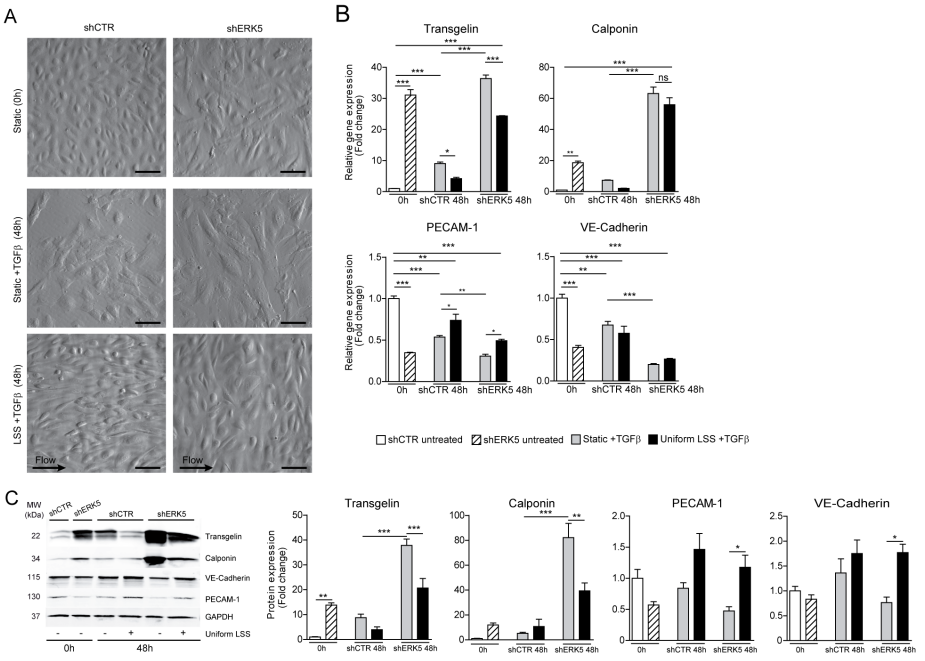

Figure 4. ERK5 gene silencing induces endothelial-to-mesenchymal transition. HUVEC were stably transduced with a short hairpin construct directed against ERK5 (shERK5) or with a non-targeting control (shCTR) and stimulated with 5 ng ml^{-1} TGFβ1 for 48 h under static conditions or with exposure to 20 dyne cm^{-2} of LSS. **(A)** Phase contrast images showing spontaneous morphological changes in HUVEC shERK5 and comparable to static HUVEC shCTR after 48 h of stimulation with TGFβ1. LSS induced alignment of HUVEC shCTR, which was less apparent with HUVEC shERK5. Scale bars: 10 µm **(B)** Mesenchymal and endothelial gene expression levels were determined by quantitative RT-PCR, and expression was related to untreated control HUVEC. Transgelin and calponin gene transcript levels were strongly upregulated in untreated HUVEC shERK5, which was even further increased after stimulation with TGFβ1. Expression of PECAM-1 and VE-Cadherin was reduced in HUVEC shERK5. Exposure to LSS partially restored the HUVEC shERK5 gene expression levels. **(C)** Representative immunoblots and quantification of endothelial and mesenchymal markers in HUVEC stably transduced with a short hairpin construct directed against ERK5 (shERK5) or with a non-targeting control (shCTR) and stimulated with 5 ng ml^{-1} TGFβ1 under static conditions (–) or with exposure to 20 dyne cm^{-2} of uniform LSS (+) for 48 h. n=3. *P* values were calculated using one-way ANOVA followed by Bonferroni's post-hoc comparisons tests. * $P < 0.05$, ** $P < 0.01$, and *** $P < 0.001$.

uniform LSS (Supplementary materials, Figure S3), we found sustained activation of ERK5 in EC from 15 min up to at least 48 h of exposure to uniform LSS (Figure 3). Consequently, downstream effectors of ERK5, *i.e.* Kruppel-like factor (KLF) 2[21] and 4[23] were induced, both on gene-transcript levels (Figure 2B) and protein-expression levels (Figure 3). HAEC showed similar induction of KLF2 and KLF4 gene-transcript levels after exposure to uniform LSS (Supplementary materials, Figure S2B). To further explore the role for ERK5 signalling in EndMT inhibition, EC were transduced with a short hairpin construct directed against ERK5 (Figure 4 and Supplementary materials, Figure S4). ERK5 silencing caused spontaneous morphological changes suggestive for EndMT, which became more apparent with TGFβ1 stimulation (Figure 4A). These observations were confirmed by the upregulation of mesenchymal markers transgelin and calponin, which was only partially inhibited by exposure to uniform LSS (Figure 4B and C). To establish the significance of ERK5 signalling in inhibition of EndMT, we expressed a constitutively active mutant of its MAP kinase MEK5 (MEK5D) in EC[23] (Figure 5 and Supplementary materials, Figure S5). MEK5D-transduced EC were resistant to TGFβ1-induced EndMT under static conditions, similar to non-transduced EC exposed to uniform LSS. EC transduced with MEK5D retained a confluent monolayer and showed no signs of hypertrophy (Figure 5A). Endothelial markers were retained and mesenchymal markers were not induced in MEK5D-transduced cells, both on gene-expression (Figure 5B) and protein-expression levels (Figure 5C). Similarly, HAEC transduced with MEK5D showed reduced transgelin and calponin gene transcript levels after stimulation with TGFβ1 compared with empty vector controls, whereas PECAM-1 gene transcript was increased in MEK5D-transduced HAEC (Supplementary materials, Figure S5A).

Since uniform LSS inhibits EndMT, we hypothesized that disturbed flow might have opposite effects. To study the differential effects of uniform LSS and disturbed flow on atherogenic differentiation, EC were exposed to LSS in Y-shaped channels which mimic the shear-stress gradients seen near arterial bifurcations. EC were protected from TGFβ1-induced EndMT in areas of uniform LSS (Figure 6A). Cells exposed to disturbed flow, present at the bifurcations and at the outer curves, showed decreased expression of VE-Cadherin and increased expression of transgelin, indicative for EndMT (Figure 6A and B). Atherogenesis is characterized by increased extracellular matrix production and deposition. Collagens form the major component of plaques of which collagen type 1 is the most prevalent isotype.[24] Areas exposed to disturbed flow showed increased collagen I deposition (Figure 6B). In more advanced stages of atherosclerosis, lesions can progress to form fibro-calcific plaques containing calcifications.[25] As EndMT can induce a stem cell-like phenotype with osteoblastic potential,[26] we studied if differential shear-stress profiles affect calcium deposition by EC cultured under osteogenic conditions. Indeed,

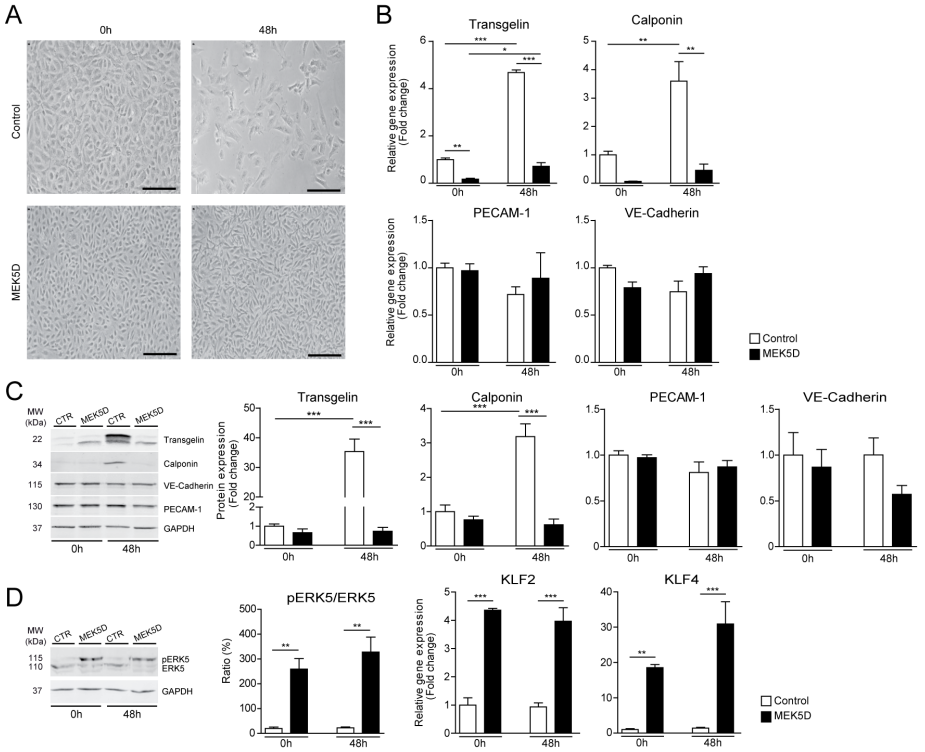

Figure 5. Constitutively active MEK5 inhibits endothelial-to-mesenchymal transition. HUVEC were stably transduced with a constitutively active mutant of MEK5 (MEK5D) or empty vector control (Control) and stimulated with 5ng ml^{-1} TGFβ1 under static conditions for 48 h. **(A)** Brightfield images showing hypertrophy in control HUVEC stimulated with TGFβ1 while HUVEC transduced with MEK5D showed no evidence of hypertrophy and retained a confluent monolayer. Scale bars: 20 µm. **(B)** Mesenchymal and endothelial gene expression levels were determined by quantitative RT-PCR, and expression was related to untreated control HUVEC. Gene transcript levels of transgelin and calponin were strongly increased in control HUVEC treated with TGFβ1 which was not seen in HUVEC transduced with MEK5D. **(C)** Representative immunoblots and quantification of endothelial and mesenchymal markers in HUVEC stably transduced with a constitutive active mutant of MEK5 (MEK5D) or empty vector control (Ctrl) and stimulated with 5ng ml^{-1} TGFβ1 under static conditions for 48 h. In contrast to control cells, mesenchymal proteins transgelin and calponin were not induced by stimulation with TGFβ1 in MEK5D. n=3. **(D)** Representative immunoblots and quantification of increased ERK5 activation in HUVEC transduced with MEK5D. Relative gene expression levels of downstream effectors KLF2 and KLF4 were also strongly increased. n=3. *P* values were calculated using one-way ANOVA followed by Bonferroni's post-hoc comparisons tests. * $P < 0.05$, ** $P < 0.01$, and *** $P < 0.001$.

calcium deposition was found in areas exposed to disturbed flow (Figure 6B). EC with constitutively active MEK5 were protected from EndMT, also in areas exposed to disturbed flow (Figure 6C), failed to produce significant amounts of collagen I and did not show any calcium deposition (Figure 6C). Thus, atherogenic differentiation can be triggered in EC exposed to disturbed flow, and ERK5 activation can inhibit this process.

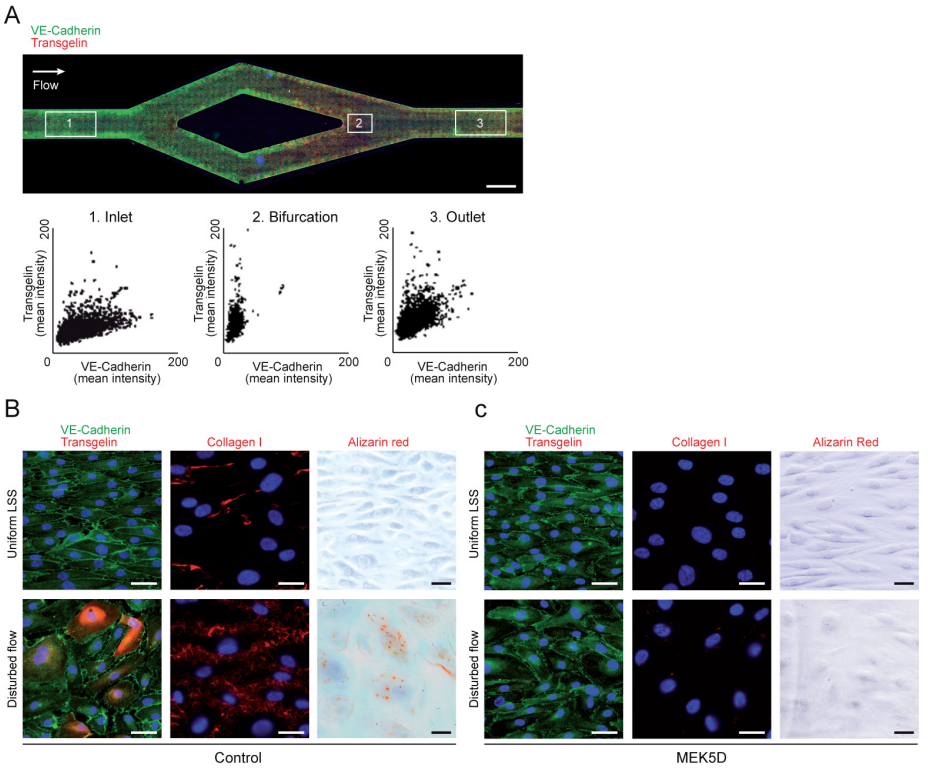

Figure 6. Disturbed flow induces atherogenic differentiation of endothelial cells. HUVEC were cultured in Y-shaped flow channels. The inlet (1) and outlet (3) of the channel are characterized by uniform LSS, whereas the area around the bifurcation (2) is characterized by disturbed flow. **(A)** HUVEC were exposed to LSS in Y-shaped channels and concomitantly stimulated with 5 ng ml^{-1} TGFβ1 for 4 days. The expression of VE-Cadherin (green) and transgelin (red) was analysed using TissueFAXS. Nuclei are stained with DAPI (blue). Scale bar: 5 mm. **(B & C)** Higher magnification images of HUVEC stably transduced with empty vector (Control) or a constitutive active mutant of MEK5 (MEK5D). Cells were exposed to LSS in Y-shaped channels and concomitantly stimulated with 5 ng ml^{-1} TGFβ1 for 4 days and analysed for VE-Cadherin (green) and transgelin (red) expression or deposition of collagen I (red). Nuclei are stained with DAPI (blue). To assess calcium deposition (red), cells were cultured in osteogenic medium for 6 days and analysed by Alizarin Red staining. Scale bars: 5 µm. n=3.

Finally, to gain additional evidence to support that disturbed flow can induce EndMT *in vivo*, mice were subjected to transverse thoracic-aortic constriction, resulting in a narrowed lumen with disturbed blood flow (Figure 7A). In the vicinity of the ligation, which is characterized by disturbed flow, the endothelial

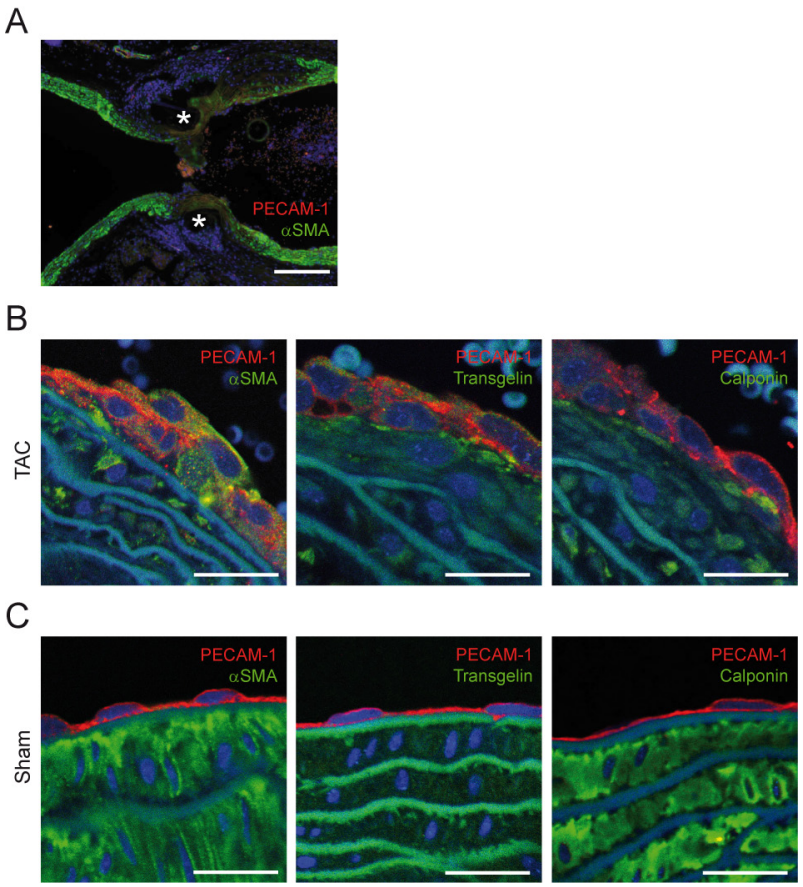

Figure 7. Disturbed flow induces endothelial-to-mesenchymal transition in vivo. Mice were subjected to transverse thoracic-aortic constriction (TAC) or sham operation (Sham). Eight weeks after surgery, the thoracic-aortic tissues were explanted and analysed for co-expression of endothelial marker PECAM-1, and mesenchymal markers αSMA, transgelin, and calponin, by confocal microscopy. **(A)** Representative stitched widefield images of αSMA (green) and PECAM-1 (red) showing the area of constriction. *Ligation. Scale bar: 200 µm. **(B)** In the vicinity of the constriction, cells co-express PECAM-1 (red) and αSMA, transgelin, and calponin (all in green). Nuclei are stained with DRAQ5 (blue). Scale bars: 20 µm. n=5 **(C)** Sham-operated animals show a normal endothelial lining (red) negative for mesenchymal protein expression (green). Nuclei are stained with DRAQ5 (blue). Scale bars: 20 µm. n=3.

lining showed drastic remodelling with loss of the typical endothelial monolayer architecture (Figure 7B). EC overlaid each other and co-expressed PECAM-1 with mesenchymal markers αSMA, transgelin, and calponin, reminiscent of EndMT (Figure 7B). Sham-operated mice showed intact endothelial monolayers, negative for mesenchymal marker expression (Figure 7C).

Discussion

Our data suggest that EndMT occurs in fibro-proliferative vascular disease and that it contributes to neointimal hyperplasia and atherogenic differentiation of EC. Importantly, we uncovered that EndMT is modulated by shear stress in an ERK5-dependent manner. Thereby, we identified a novel atheroprotective mechanism of uniform LSS, which might in part further explain the focal nature of vascular disease.

As proof-of-concept, we analysed human atherosclerotic plaques and porcine neointimal lesions for evidence of EndMT and identified myo-EC in intermediate stages of transition.[27] This corroborates earlier suggestions of a role for EndMT in neointimal thickening.[14,15] This was recently confirmed by Cooley *et al.*[28] by using lineage tracing strategies to study the contribution of different cell types to the neointima formation during vein graft remodelling. They observed that 51.7±3.3% of the neointimal cells were of endothelial origin.[28] In addition, Yao *et al.*[29] showed that EndMT contributes to vascular calcification. Together, these data clearly indicate that EndMT contributes to vascular disease. In the human and porcine tissues we analysed, the presence of myo-EC was confined to regions with disturbed shear stress. To further substantiate a role for EndMT in neointimal hyperplasia and to study its relation to disturbed shear stress, we experimentally induced disturbed flow in the murine thoracic aorta using thoracic-aortic constriction. While there was no evidence for EndMT in the sham-operated mice, myo-EC were present in the areas exposed to disturbed flow. Since these observations lack spatiotemporal resolution, we cannot rule out that the myo-EC arise through other mechanisms than EndMT. Earlier studies have shown the formation of a (pseudo)endothelium by smooth muscle cells after endothelial denudation, although these cells did not co-express endothelial markers.[30,31] The porcine tissues used in this study were obtained from healthy, untreated animals and myo-EC were observed throughout the neointima, not only at the innermost lining. Likewise, the thoracic-aortic constriction procedure in mice does not result in endothelial denudation, and also here the neointimal cells co-expressed endothelial PECAM-1, making this explanation less likely. It is, however, well established that media-derived smooth muscle cells contribute to neointima formation.[1] In this regard, EndMT might not only provide neointimal cells, but

also act on migration and proliferation of smooth muscle cells through enhanced paracrine signalling.[8] Recently, Qiao *et al.*[32] demonstrated that the neointimal cells in experimental pulmonary hypertension, are partially derived from the endothelial lineage. However, using a different experimental model for the same disease, Sheikh *et al.*[33] showed that pathological muscularization of distal arterioles mainly involves migration and proliferation of pre-existing smooth muscle cells. This suggests that the mechanisms underlying these processes are distinct, which is supported by the fact that medial hypertrophy precedes the development of neointimal lesions in pulmonary hypertension.[34] The origin of fibro-proliferative cells is presumably vessel dependent, and influenced by local differences in haemodynamic forces such as shear stress or cyclic strain, as well as other microenvironmental cues such as oxygen tension levels. Most likely, these processes are intertwined and additional lineage-tracing analyses are needed to address the spatiotemporal relationship between these cells and processes.

Importantly, our data uncovered a novel atheroprotective mechanism of shear stress, namely ERK5-mediated inhibition of EndMT, which in part can explain the focal nature of fibro-proliferative vascular disease. High LSS resulted in activation of ERK5 and inhibition of EndMT and atherogenic differentiation. While these processes were induced by disturbed flow, this could be inhibited by activation of ERK5. Earlier studies have shown that LSS is associated with quiescent, anti-inflammatory, and anti-thrombogenic endothelium, which is mainly accredited to activation of the MEK5/ERK5 cascade.[20-22] As a mechano-activated downstream effector of MEK5/ERK5, many of the vasculoprotective effects of shear stress have been attributed to KLF2.[21,35,36] Ohnesorge *et al.*[23] have shown that KLF4, another MEK5/ERK5 effector, has vasculoprotective effects similar to KLF2, in agreement with other data showing mechanistic and functional conservation between KLF2 and KLF4.[37] Interestingly, KLF4 plays a pivotal role in the regulation of smooth muscle plasticity by acting as a potent transcriptional repressor of SM differentiation. KLF4 supresses myocardin expression, a potent co-activator of serum response factor (SRF)[38] and prevents SRF/myocardin from associating with SM gene promoters.[39] Transcription of SM genes is also repressed by KLF4 through direct binding to transforming growth factor-β control elements (TCE) in promoter regions of SMC differentiation genes[40] and by inhibiting binding of Smad3 to Smad binding elements (SBE).[41] In epithelial-to-mesenchymal transition (EMT), which has been studied more extensively than EndMT, KLF4 inhibits transition through transcriptional activation of E-cadherin[42] and suppression of Snail,[43] a suppressor of E-Cadherin and important inducer of EMT.[44] Interestingly, KLF4 also transcriptionally regulates VE-Cadherin.[45] Since KLF4 can inhibit EndMT via multiple mechanisms, the inhibitory effects of ERK5 signalling on EndMT are likely mediated through KLF4. However, recent data indicate that

KLF2, not KLF4, inhibits the enhanced migration of EC associated with fibro-proliferative vascular disease.[46] KLF2 and KLF4 might thus act in concert in the inhibition of EndMT, which should be addressed in future studies.

Our findings suggest that inhibition of EndMT might provide a novel therapeutic strategy to treat fibro-proliferative vascular disease by suppressing neointimal hyperplasia and atherogenic differentiation. Selective ERK5 agonists are required to determine the efficacy of ERK5 activation in inhibition of EndMT *in vivo*. From a clinical perspective, re-differentiation of fibro-proliferative cells to EC is also highly relevant, as it potentially enforces regression of disease by restoring vascular homeostasis. Remarkably, although reversion of epithelial cells through a process termed mesenchymal-to-epithelial transition (MET) is well established,[47] reversal of EndMT has not been described as yet. Recent data indicate that cardiac fibroblasts undergo mesenchymal-to-endothelial transition to enhance neovascularization in the injured heart through enhanced p53 signalling.[48] Intriguingly, prolonged exposure of EC to LSS results in sustained activation of p53 and growth arrest.[49] Moreover, KLF4 physically interacts with p53 in synergistic activation of p21, indicating interaction between p53 and ERK5 signalling pathways.[50] Activation of ERK5 thus not only inhibits mesenchymal transition of EC, but might also be the key to reversal of the transition process, which would provide exciting new perspectives on the treatment of cardiovascular disease and cardiovascular regeneration and should be addressed in future studies.

Acknowledgements

We thank C.N. Belterman, J.M.T. de Bakker (AMC, University of Amsterdam), and M. Parvizi (Department of Pathology & Medical Biology, UMCG) for help with the porcine tissues; A.R. de Jong, I. Kuipers, and I. Vreeswijk-Baudoin (Department of Experimental Cardiology, UMCG) for help with the aortic banding; Imaging was performed at the UMCG Imaging Center (UMIC), supported by the Netherlands Organization for Health Research and Development (ZonMW grant 40-00506-98-9021).

Funding

This work was supported by the Groningen University Institute for Drug Exploration (GUIDE) (to J.-R.M., M.M., G.K., M.H.); the W.J. Kolff Institute (to E.S.L. and M.H.); the Netherlands Heart Foundation (Grant 2013T116 to J.-R.M.); the ZonMW/NWO Innovational Research Incentive grant (no. 916.11.022 to G.K.); the JK de Cock Foundation (to J.-R.M. and E.S.L.), and the Translational Excellence in Regenerative Medicine (TeRM) Smart Mix

Program of the Netherlands Ministry of Economic Affairs and the Netherlands Ministry of Education, Culture and Science (to J.-R.M. and M.H.).

References

1. Ross R and Glomset JA. Atherosclerosis and the arterial smooth muscle cell: proliferation of smooth muscle is a key event in the genesis of the lesions of atherosclerosis. *Science.* 1973;180:1332–1339.
2. Chatzizisis YS, Coskun AU, Jonas M, Edelman ER, Feldman CL and Stone PH. Role of endothelial shear stress in the natural history of coronary atherosclerosis and vascular remodeling: molecular, cellular, and vascular behavior. *J Am Coll Cardiol.* 2007;49:2379–2393.
3. Zarins CK, Giddens DP, Bharadvaj BK, Sottiurai VS, Mabon RF and Glagov S. Carotid bifurcation atherosclerosis. Quantitative correlation of plaque localization with flow velocity profiles and wall shear stress. *Circ Res.* 1983;53:502–514.
4. Cunningham KS and Gotlieb AI. The role of shear stress in the pathogenesis of atherosclerosis. *Lab Invest.* 2005;85:9–23.
5. Nackman GB, Fillinger MF, Shafritz R, Wei T and Graham AM. Flow modulates endothelial regulation of smooth muscle cell proliferation: a new model. *Surgery.* 1998;124:353–360.
6. Krenning G, Moonen JR, van Luyn MJ and Harmsen MC. Vascular smooth muscle cells for use in vascular tissue engineering obtained by endothelial-to-mesenchymal transdifferentiation (EnMT) on collagen matrices. *Biomaterials.* 2008;29:3703–3711.
7. Maleszewska M, Moonen JR, Huijkman N, van de Sluis B, Krenning G and Harmsen MC. IL-1beta and TGFbeta2 synergistically induce endothelial to mesenchymal transition in an NFkappaB-dependent manner. *Immunobiology.* 2013;218:443–454.
8. Moonen JR, Krenning G, Brinker MG, Koerts JA, van Luyn MJ and Harmsen MC. Endothelial progenitor cells give rise to pro-angiogenic smooth muscle-like progeny. *Cardiovasc Res.* 2010;86:506–515.
9. van Meeteren LA and ten Dijke P. Regulation of endothelial cell plasticity by TGF-beta. *Cell Tissue Res.* 2012;347:177–186.
10. Markwald RR, Fitzharris TP and Manasek FJ. Structural development of endocardial cushions. *Am J Anat.* 1977;148:85–119.
11. Zhu P, Huang L, Ge X, Yan F, Wu R and Ao Q. Transdifferentiation of pulmonary arteriolar endothelial cells into smooth muscle-like cells regulated by myocardin involved in hypoxia-induced pulmonary vascular remodelling. *Int J Exp Pathol.* 2006;87:463–474.
12. Zeisberg EM, Tarnavski O, Zeisberg M, Dorfman AL, McMullen JR, Gustafsson E, Chandraker A, Yuan X, Pu WT, Roberts AB, Neilson EG, Sayegh MH, Izumo S and Kalluri R. Endothelial-to-mesenchymal transition contributes to cardiac fibrosis. *Nat Med.* 2007;13:952–961.
13. Zeisberg EM, Potenta SE, Sugimoto H, Zeisberg M and Kalluri R. Fibroblasts in kidney fibrosis emerge via endothelial-to-mesenchymal transition. *J Am Soc Nephrol.* 2008;19: 2282–2287.
14. Beranek JT and Cavarocchi NC. Undifferentiated vascular endothelial cells in coronary allograft atherosclerosis. *Int J Cardiol.* 1990;28:127–128.
15. Beranek JT. Vascular endothelium-derived cells containing smooth muscle

actin are present in restenosis. *Lab Invest.* 1995;72:771.

16. Carrillo LM, Arciniegas E, Rojas H and Ramirez R. Immunolocalization of endocan during the endothelial-mesenchymal transition process. *Eur J Histochem.* 2011;55:e13.
17. Comerford A and David T. Computer model of nucleotide transport in a realistic porcine aortic trifurcation. *Ann Biomed Eng.* 2008;36:1175–1187.
18. Resnick N, Yahav H, Shay-Salit A, Shushy M, Schubert S, Zilberman LC and Wofovitz E. Fluid shear stress and the vascular endothelium: for better and for worse. *Prog Biophys Mol Biol.* 2003;81:177–199.
19. Markwald RR, Fitzharris TP and Smith WN. Sturctural analysis of endocardial cytodifferentiation. *Dev Biol.* 1975;42:160–180.
20. Traub O and Berk BC. Laminar shear stress: mechanisms by which endothelial cells transduce an atheroprotective force. *Arterioscler Thromb Vasc Biol.* 1998;18:677–685.
21. Parmar KM, Larman HB, Dai G, Zhang Y, Wang ET, Moorthy SN, Kratz JR, Lin Z, Jain MK, Gimbrone MA Jr and Garcia-Cardena G. Integration of flow-dependent endothelial phenotypes by Kruppel-like factor 2. *J Clin Invest.* 2006;116:49–58.
22. Yan C, Takahashi M, Okuda M, Lee JD and Berk BC. Fluid shear stress stimulates big mitogen-activated protein kinase 1 (BMK1) activity in endothelial cells. Dependence on tyrosine kinases and intracellular calcium. *J Biol Chem.* 1999;274:143–150.
23. Ohnesorge N, Viemann D, Schmidt N, Czymai T, Spiering D, Schmolke M, Ludwig S, Roth J, Goebeler M and Schmidt M. Erk5 activation elicits a vasoprotective endothelial phenotype via induction of Kruppel-like factor 4 (KLF4). *J Biol Chem.* 2010;285:26199–26210.
24. McCullagh KA and Balian G. Collagen characterisation and cell transformation in human atherosclerosis. *Nature.* 1975;258:73–75.
25. Johnson RC, Leopold JA and Loscalzo J. Vascular calcification: pathobiological mechanisms and clinical implications. *Circ Res.* 2006;99:1044–1059.
26. Medici D, Shore EM, Lounev VY, Kaplan FS, Kalluri R and Olsen BR. Conversion of vascular endothelial cells into multipotent stem-like cells. *Nat Med.* 2010;16:1400–1406.
27. Zeisberg EM, Potenta S, Xie L, Zeisberg M and Kalluri R. Discovery of endothelial to mesenchymal transition as a source for carcinoma-associated fibroblasts. *Cancer Res.* 2007;67:10123–10128.
28. Cooley BC, Nevado J, Mellad J, Yang D, St HC, Negro A, Fang F, Chen G, San H, Walts AD, Schwartzbeck RL, Taylor B, Lanzer JD,Wragg A, Elagha A, Beltran LE, Berry C, Feil R, Virmani R, Ladich E, Kovacic JC and Boehm M. TGF-beta signaling mediates endothelial-to-mesenchymal transition (EndMT) during vein graft remodeling. *Sci Transl Med.* 2014;6:227ra34.
29. Yao Y, Jumabay M, Ly A, Radparvar M, Cubberly MR and Boström KI. A role for the endothelium in vascular calcification. *Circ Res.* 2013;113:495–504.
30. Clowes AW, Collazzo RE and Karnovsky MJ. A morphologic and permeability study of luminal smooth muscle cells after arterial injury in the rat. *Lab Invest.* 1978;39:141–150.
31. Clowes AW, Clowes MM and Reidy MA. Kinetics of cellular proliferation after arterial injury. III. Endothelial and smooth muscle growth in chronically denuded vessels. *Lab Invest.* 1986;54:295–303.
32. Qiao L, Nishimura T, Shi L, Sessions D, Thrasher A, Trudell JR, Berry GJ, Pearl RG and Kao PN. Endothelial fate mapping in mice with pulmonary hypertension. *Circulation.* 2014;129:692–703.

33. Sheikh AQ, Lighthouse JK and Greif DM. Recapitulation of developing artery muscularization in pulmonary hypertension. *Cell Rep.* 2014;6:809–817.

34. Dickinson MG, Bartelds B, Borgdorff MA and Berger RM. The role of disturbed blood flow in the development of pulmonary arterial hypertension: lessons from preclinical animal models. *Am J Physiol Lung Cell Mol Physiol.* 2013;305:L1–L14.

35. Dekker RJ, van Soest S, Fontijn RD, Salamanca S, de Groot PG, VanBavel E, Pannekoek H and Horrevoets AJ. Prolonged fluid shear stress induces a distinct set of endothelial cell genes, most specifically lung Kruppel-like factor (KLF2). *Blood.* 2002;100:1689–1698.

36. Lee JS, Yu Q, Shin JT, Sebzda E, Bertozzi C, Chen M, Mericko P, Stadtfeld M, Zhou D, Cheng L, Graf T, MacRae CA, Lepore JJ, Lo CW and Kahn ML. Klf2 is an essential regulator of vascular hemodynamic forces in vivo. *Dev Cell.* 2006;11:845–857.

37. Villarreal G Jr, Zhang Y, Larman HB, Gracia-Sancho J, Koo A and Garcia-Cardena G. Defining the regulation of KLF4 expression and its downstream transcriptional targets in vascular endothelial cells. *Biochem Biophys Res Commun.* 2010;391:984–989.

38. Wang Z, Wang DZ, Pipes GC and Olson EN. Myocardin is a master regulator of smooth muscle gene expression. *Proc Natl Acad Sci U S A.* 2003;100:7129–7134.

39. Liu Y, Sinha S, McDonald OG, Shang Y, Hoofnagle MH and Owens GK. Kruppel-like factor 4 abrogates myocardin-induced activation of smooth muscle gene expression. *J Biol Chem.* 2005;280:9719–9727.

40. Adam PJ, Regan CP, Hautmann MB and Owens GK. Positive- and negative-acting Kruppel-like transcription factors bind a transforming growth factor beta control element required for expression of the smooth muscle cell differentiation marker SM22alpha in vivo. *J Biol Chem.* 2000;275:37798–37806.

41. Hu B, Wu Z, Liu T, Ullenbruch MR, Jin H and Phan SH. Gut-enriched Kruppel-like factor interaction with Smad3 inhibits myofibroblast differentiation. *Am J Respir Cell Mol Biol.* 2007;36:78–84.

42. Yori JL, Seachrist DD, Johnson E, Lozada KL, Abdul-Karim FW, Chodosh LA, Schiemann WP and Keri RA. Kruppel-like factor 4 inhibits tumorigenic progression and metastasis in a mouse model of breast cancer. *Neoplasia.* 2011;13:601–610.

43. Yori JL, Johnson E, Zhou G, Jain MK and Keri RA. Kruppel-like factor 4 inhibits epithelial-to-mesenchymal transition through regulation of E-cadherin gene expression. *J Biol Chem.* 2010;285:16854–16863.

44. Cano A, Perez-Moreno MA, Rodrigo I, Locascio A, Blanco MJ, del Barrio MG, Portillo F and Nieto MA. The transcription factor snail controls epithelial-mesenchymal transitions by repressing E-cadherin expression. *Nat Cell Biol.* 2000;2:76–83.

45. Cowan CE, Kohler EE, Dugan TA, Mirza MK, Malik AB and Wary KK. Kruppel-like factor-4 transcriptionally regulates VE-cadherin expression and endothelial barrier function. *Circ Res.* 2010;107:959–966.

46. Komaravolu RK, Adam C, Moonen JR, Harmsen MC, Goebeler M and Schmidt M. Erk5 inhibits endothelial migration via KLF2-dependent downregulation of PAK1. *Cardiovasc Res.* 2015;105:86–95.

47. Kalluri R. EMT: when epithelial cells decide to become mesenchymal-like cells. *J Clin Invest.* 2009;119:1417–1419.

48. Ubil E, Duan J, Pillai IC, Rosa-Garrido M, Wu Y, Bargiacchi F, Lu Y, Stanbouly S, Huang J, Rojas M, Vondriska TM,

Stefani E and Deb A. Mesenchymal-endothelial transition contributes to cardiac neovascularization. *Nature.* 2014;514:585–590.

49. Lin K, Hsu PP, Chen BP, Yuan S, Usami S, Shyy JY, Li YS and Chien S. Molecular mechanism of endothelial growth arrest by laminar shear stress. *Proc Natl Acad Sci U S A.* 2000;97:9385–9389.
50. Yoon HS, Chen X and Yang VW. Kruppel-like factor 4 mediates p53-dependent G1/S cell cycle arrest in response to DNA damage. *J Biol Chem.* 2003;278:2101–2105.

Supplementary materials

Supplementary methods

Immunohistochemistry – Imaging

Overview images of porcine aortic trifurcation tissue and murine thoracic-aortic constriction tissue were obtained through ×20 (Plan-Neofluar 0.4 NA, dry, Ph2) and ×40 (Plan-Neofluar, 1.30 NA, oil, DIC) objectives of an upright epifluorescence microscope (Zeiss AxioObserver Z1) and controlled by TissueFAXS (TissueGnostics GmbH, Vienna, Austria). Overview images of cells on Y-shaped slides were obtained through ×20 (Plan-Neofluar, 0.4 NA, dry, Ph2) and magnifications through ×63 (Plan-Apochromat, NA 1.40, oil, DIC) objectives using the same setup as described above and analysed using TissueQuest software (TissueGnostics GmbH, Vienna, Austria). Phase contrast images were obtained through ×10 (C Plan 0.22 NA) of an inverted contrasting microscope (Leica DM IL). Confocal images were obtained using a Leica TCS SP2 AOBS spectral confocal microscope through a ×63 (HCX PL APO 1.40 NA, oil) objective. 488 and 543 channels were scanned sequentially. Images were analysed using Imaris 7.2.1 (Bitplane AG, Zürich, Switzerland), z-stacks were created using ImageJ version 1.43u (NIH, USA).

Supplementary tables

Table S1. Antibodies used for immunohistochemistry

antigen	supplier	dilution
αSMA	#5694, Abcam, UK	1:200
	#7817, Abcam, UK	1:200
calponin	#46794, Abcam, UK	1:200
collagen I	#34710, Abcam, UK	1:400
endocan	LIA-0901, Lunginnov, France	1:200
FSP-1	#27957, Abcam, UK	1:250
PECAM-1	M0823, Dako, Belgium	1:30
	#1506 Santa Cruz Biotechnology, CA	1:200
transgelin	#14106, Abcam, UK	1:200
VE-cadherin	MAB9381, R&D systems, MN	1:400
anti-Mouse TRITC	#1031-03, Southern Biotech, AL	1:200
anti-Mouse Alexa 488	#A21202, Life Technologies, The Netherlands	1:300
anti-Mouse Alexa 546	#A11003, Life Technologies, The Netherlands	1:300
anti-Rabbit Alexa 488	#A21206, Life Technologies, The Netherlands	1:300
anti-Rabbit Alexa 555	#A31572, Life Technologies, The Netherlands	1:300
anti-Rabbit Alexa 594	#A21207, Life Technologies, The Netherlands	1:300
anti-Goat Alexa 555	#A21431, Life Technologies, The Netherlands	1:300
DRAQ5	#4084, Cell Signaling, CA	1:1000

Table S2. Antibodies used for immunoblotting

antigen	supplier	dilution
αSMA	#5694, Abcam, UK	1:200
calponin	#46794, Abcam, UK	1:1000
GAPDH	#8345, Abcam, UK	1:2000
	#9485, Abcam, UK	1:2000
KLF2	sc-28675, Santa Cruz Biotechnology, CA	1:500
KLF4	sc-20691, Santa Cruz Biotechnology, CA	1:500
PECAM-1	#28364, Abcam, UK	1:500
transgelin	#14106, Abcam, UK	1:1000
VE-Cadherin	#2500, Cell Signalling, CA	1:1000
ERK1/2	#4695, Cell Signalling, CA	1:500
phospho-ERK1/2	#9101, Cell Signalling, CA	1:500
ERK5	#07-039, Millipore, MA	1:500
p38 MAPK	#9212, Cell Signalling, CA	1:500
phospho-p38MAPK	#4731, Cell Signalling, CA	1:500
JNK	sc-7345, Santa Cruz Biotechnology, CA	1:500
phospho-JNK	#9255, Cell Signalling, CA	1:500
anti-Rb IRDye 680	#926-68073, LI-COR Biosciences, Germany	1:10000
anti-Ms IRDye 800	#926-32212, LI-COR Biosciences, Germany	1:10000

Table S3. Primer sequences

gene name		primer sequence
β2M	F	TTCTGGCCTGGAGGCTATC
	R	TCAGGAAATTTGACTTTCCATTC
transgelin	F	CTGAGGACTATGGGGTCATC
	R	TAGTGCCCATCATTCTTGGT
calponin	F	TGAAGTACGCAGAGAAGCAG
	R	CAGCTTGGGGTCGTAGAG
VE-cadherin	F	AAGCCTCTGATTGGCACAGT
	R	CTGGCCCTTGTCACTGGT
PECAM-1	F	GTGAGGGTCAACTGTTCTGT
	R	GTGACCAGTTCACTCTTGGT
KLF2	F	CATCTGAAGGCGCATCTG
	R	CGTGTGCTTTCGGTAGTGG
KLF4	F	GGGAGAAGACACTGCGTCA
	R	GGAAGCACTGGGGGAAGT

Supplementary figures

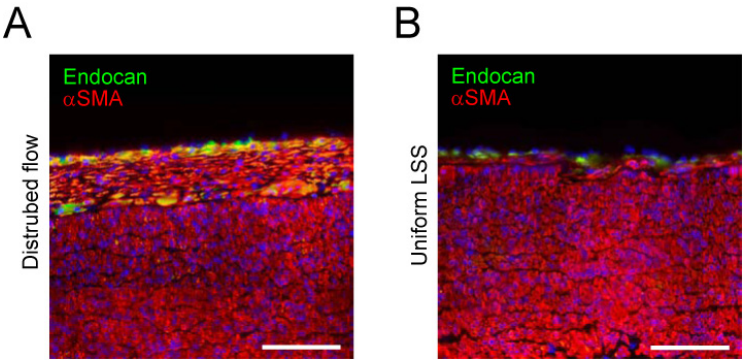

Figure S1. Stitched widefield images of regions exposed to uniform LSS and disturbed flow in porcine abdominal aortic trifurcation. (A) A neointimal lesion containing cells co-expressing endocan (green) and αSMA (red) is present in the region exposed to disturbed flow. **(B)** No neointimal lesion is present in the region exposed to uniform LSS; endothelial cells stain for endocan (green) and medial smooth muscle cells for αSMA (red). Nuclei are stained with DAPI (blue). Scale bars: 150 µm.

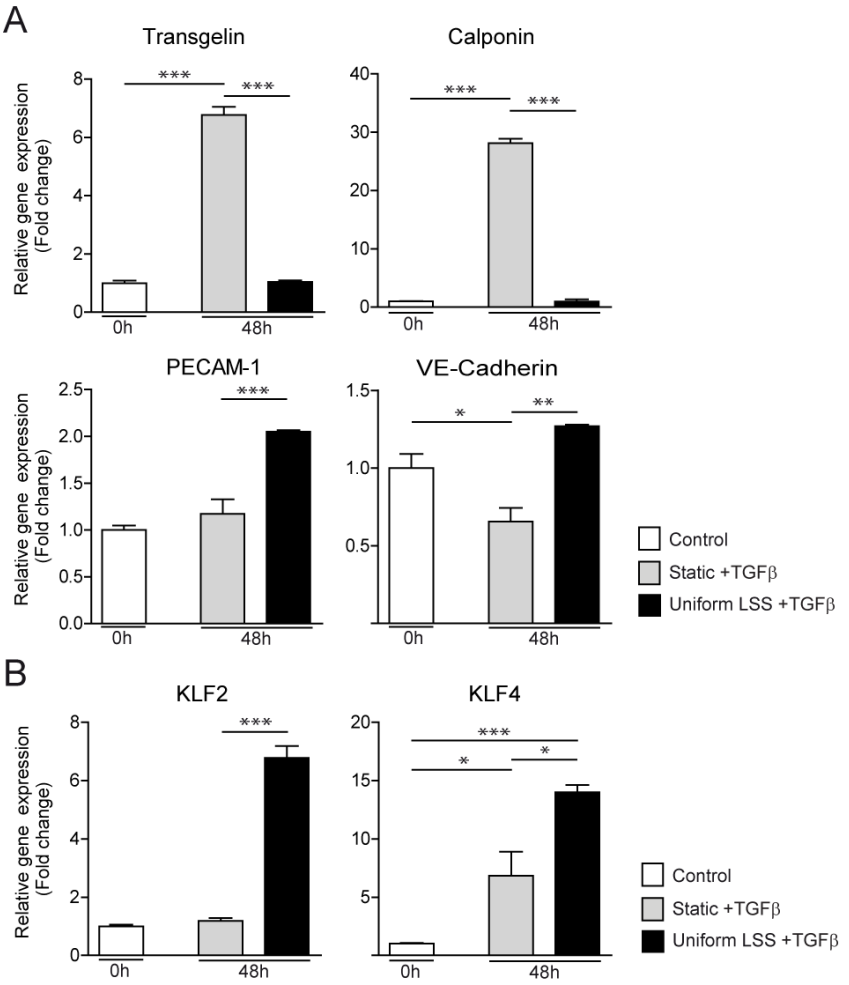

Figure S2. Laminar shear stress (LSS) inhibits endothelial-to-mesenchymal transition of HAEC. Human aortic endothelial cells (HAEC) were stimulated with 5 ng ml^{-1} TGFβ1, both under static conditions and with exposure to 20 dyne cm^{-2} of LSS for 48 h. **(A)** Mesenchymal and endothelial gene expression levels were determined by quantitative RT-PCR, and expression was related to untreated control HAEC. Under static conditions, expression of transgelin and calponin is increased. Although PECAM-1 gene transcript is increased by stimulation with TGFβ1, VE-Cadherin expression is reduced when stimulated under static conditions. **(B)** Relative gene expression levels of KLF2 and KLF4 were increased in HAEC by exposure to LSS at 48 h. n=3. *P* values were calculated using one-way ANOVA followed by Bonferroni's post-hoc comparisons tests. * $P < 0.05$, ** $P < 0.01$, and *** $P < 0.001$.

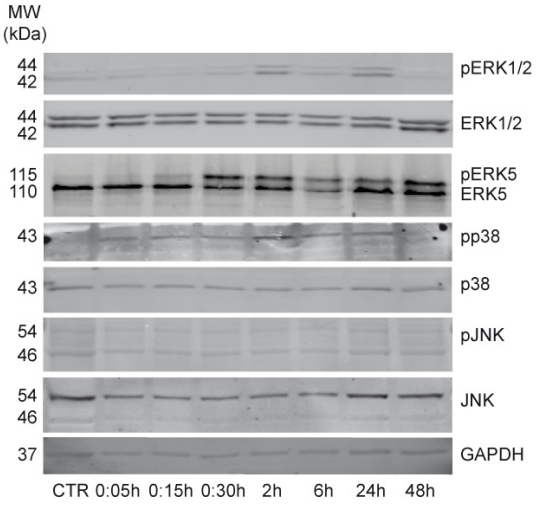

Figure S3. Activation of MAPK signalling pathways by LSS. HUVEC were exposed to 20 dyne cm^{-2} of LSS for up to 48 h. Activation status, *i.e.* phosphorylation of ERK1/2, ERK5, p38 and JNK was determined at the indicated time points by immunoblotting. Representative immunoblot shows transient activation for ERK1/2, p38 and JNK. Only ERK5 showed sustained activation for at least 48 h. n=3.

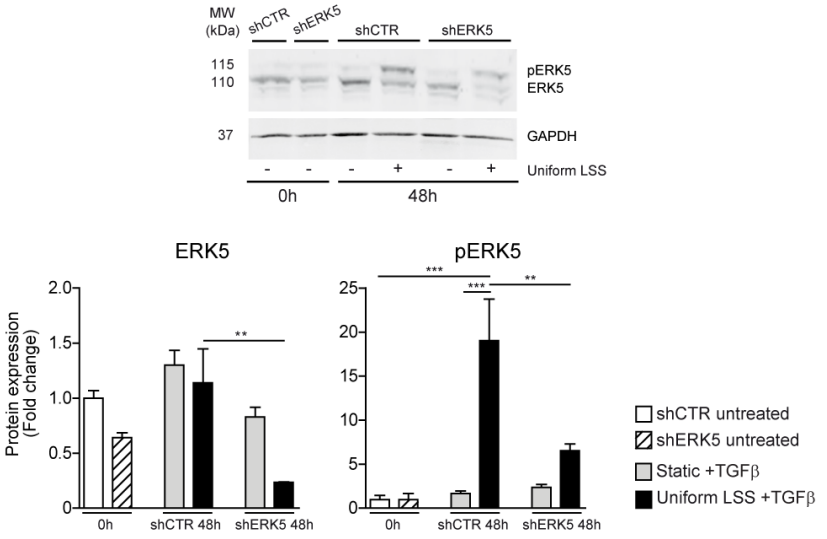

Figure S4. ERK5 gene silencing induces endothelial-to-mesenchymal transition. HUVEC were stably transduced with a short hairpin construct directed against ERK5 (shERK5) or with a non-targeting control (shCTR) and stimulated with 5 ng ml^{-1} TGFβ1 for 48 h under static conditions or with exposure to 20 dyne cm^{-2} of LSS. Representative immunoblot and quantification of laminar flow-induced activation of ERK5. n=3. *P* values were calculated using one-way ANOVA followed by Bonferroni's post-hoc comparisons tests. ** $P < 0.01$, and *** $P < 0.001$.

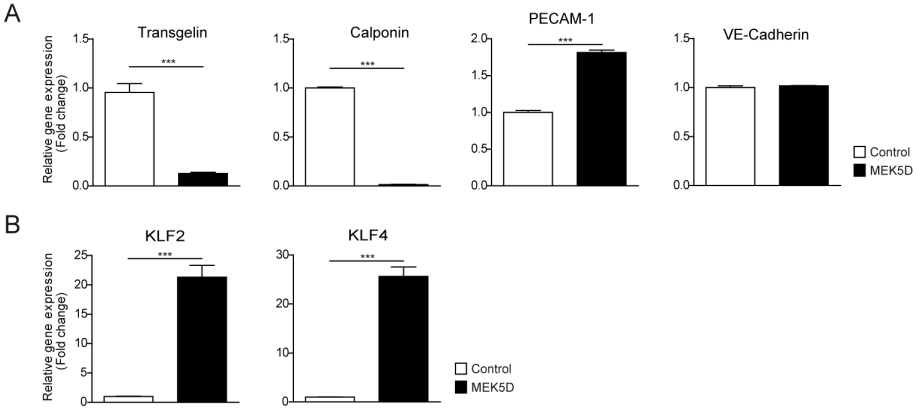

Figure S5. Constitutively active MEK5 inhibits endothelial-to-mesenchymal transition of HAEC. HAEC were transduced with a constitutively active mutant of MEK5 (MEK5D) or empty vector control (Control) and stimulated with 5ng ml^{-1} TGFβ1 under static conditions for 48 h. **(A)** Mesenchymal and endothelial gene expression levels were determined by quantitative RT-PCR. Transgelin and calponin gene transcript levels were strongly decreased in HAEC transduced with MEK5D compared to empty vector controls, whereas PECAM-1 gene transcript was increased in MEK5D transduced cells. **(B)** Relative gene expression levels of KLF2 and KLF4 were also increased in HAEC transduced with MEK5D. n=3. *P* values were calculated by unpaired t test. *** *P* <0.001.